

## Dynamical emission of phonon pairs in optomechanical systems

Fen Zou<sup>⊗</sup>,<sup>1</sup> Jie-Qiao Liao,<sup>2,3,\*</sup> and Yong Li<sup>⊗</sup><sup>1,3,4,†</sup>

<sup>1</sup>Beijing Computational Science Research Center, Beijing 100193, China

<sup>2</sup>Key Laboratory of Low-Dimensional Quantum Structures and Quantum Control of Ministry of Education, Key Laboratory for Matter Microstructure and Function of Hunan Province, Department of Physics, Hunan Normal University, Changsha 410081, China

<sup>3</sup>Synergetic Innovation Center for Quantum Effects and Applications, Hunan Normal University, Changsha 410081, China

<sup>4</sup>Center for Theoretical Physics and School of Science, Hainan University, Haikou 570228, China



(Received 20 January 2022; revised 10 April 2022; accepted 27 April 2022; published 10 May 2022)

The multiphonon state plays an important role in quantum information processing and quantum metrology. Here we propose a scheme to realize dynamical emission of phonon pairs based on the technique of stimulated Raman adiabatic passage in a single-cavity optomechanical system, where the optical cavity is driven by two Gaussian pulse lasers. By exploring quantum trajectories of the state populations and the average phonon number, we find that the dynamical phonon-pair emission can be realized under the appropriate parameter conditions and is tunable by controlling the time interval between the consecutive pulses of pump lasers. In particular, the numerical results for the standard and generalized second-order correlation functions of the mechanical mode show that the system can behave as an antibunched phonon-pair emitter. Our proposal can be extended to achieve an antibunched  $n$ -phonon emitter, which has potential applications for on-chip quantum communication.

DOI: [10.1103/PhysRevA.105.053507](https://doi.org/10.1103/PhysRevA.105.053507)

### I. INTRODUCTION

The realization of the nonclassical states has become an interesting and important research topic in quantum information science, with potential applications in quantum communication [1], quantum metrology [2], quantum lithography [3], quantum spectroscopy [4,5], and quantum biology [6,7]. Recently, the generation of  $n$ -quanta states has been studied theoretically in multilevel atomic systems [8–17], Rydberg atomic ensembles [18,19], cavity quantum electrodynamics (QED) systems [20–31], circuit QED systems [32], waveguide QED systems [33–35], Kerr cavity systems [36,37], and cavity optomechanical systems [38]. In particular, an emitter of  $n$ -photon bundles, releasing their energy in the bundle of  $n$  photons, was first proposed by Sánchez Muñoz *et al.* in a cavity QED system [20].

Subsequently, a series of schemes on the  $n$ -photon and  $n$ -phonon bundle emissions have been proposed in a variety of quantum systems, e.g., cavity [22–27] and circuit QED systems [32]. The antibunched  $n$ -photon and  $n$ -phonon bundle emissions can be used to realize multiphoton and multiphonon sources [39,40], respectively. However, since the high-order process of the single-photon (single-phonon) transition is generally very weak, the experimental realization of the multiphoton (multiphonon) state is still a challenge.

In this work, we propose a scheme for implementing dynamical phonon-pair emission in a cavity optomechanical system composed of an optical cavity and a mechanical resonator [41–46], where the optical cavity is driven by two

Gaussian pulse lasers. Under the appropriate parameter conditions, the dimensions of the Hilbert space of the cavity and mechanical modes are truncated up to 1 and 2 excitations, respectively. Based on the technique of stimulated Raman adiabatic passage (STIRAP) [47–49], the population transfer between zero-phonon state and two-phonon state can be realized in the absence of dissipation in the system. In the presence of dissipation, we find that the dynamical phonon-pair emission can be observed by analyzing quantum trajectories of the state populations and the average phonon number in the system. In addition, we investigate quantum statistics of the dynamical phonon-pair emission by numerically calculating the standard and generalized second-order correlation functions in the mechanical mode. It can be found that the system behaves as an antibunched phonon-pair emitter when the time interval  $T$  between the consecutive pulses of pulse lasers is much larger than the mechanical lifetime  $1/\gamma_m$ , i.e.,  $\gamma_m T \gg 1$ . Particularly, compared to the previous  $n$ -phonon bundle emission [23,25], the time interval of the dynamical phonon-pair emission can be tuned by adjusting the time interval between the consecutive pulses. Our work opens up a route to achieve an antibunched phonon-pair emitter, which could be useful for quantum information processing and for medical applications.

The rest of this paper is organized as follows. In Sec. II, we introduce the physical model and present the Hamiltonian of the system. In Sec. III, we derive an effective Hamiltonian of the system in a finite-dimensional Hilbert space and analyze the generation of the two-phonon state. In Sec. IV, we study the dynamical emission of phonon pairs by analyzing quantum trajectories of the state populations and the average phonon number in the system. We also investigate the statistical properties of the dynamical phonon-pair emission by

\*Corresponding author: [jqliao@hunnu.edu.cn](mailto:jqliao@hunnu.edu.cn)

†Corresponding author: [liyong@csrc.ac.cn](mailto:liyong@csrc.ac.cn)

numerically calculating the standard and generalized second-order correlation functions in the mechanical mode. Finally, we present some discussions on the experimental parameters and conclude this work in Sec. V.

## II. MODEL AND HAMILTONIAN

As schematically shown in Fig. 1(a), we consider a cavity optomechanical system which consists of a single-cavity mode coupled to a mechanical mode via radiation-pressure interaction. The cavity is driven by two Gaussian pulse driving fields with corresponding driving carrier frequencies  $\omega_1$  and  $\omega_2$ , where each driving field is composed of a series of consecutive Gaussian wave packets. The Hamiltonian of the system reads as ( $\hbar = 1$ )

$$H = \omega_c a^\dagger a + \omega_m b^\dagger b - g a^\dagger a (b^\dagger + b) + [\Omega_1(t) a^\dagger e^{-i\omega_1 t} + \Omega_2(t) a^\dagger e^{-i\omega_2 t} + \text{H.c.}] \quad (1)$$

with the time-dependent amplitudes of the driving fields

$$\Omega_i(t) = \Omega_0 \sum_{k=0}^{\infty} \exp\left[-\frac{(t - t_i - kT)^2}{2\sigma^2}\right], \quad i = 1, 2. \quad (2)$$

Here  $a^\dagger$  ( $a$ ) is the creation (annihilation) operator of the cavity mode with resonance frequency  $\omega_c$ ,  $b^\dagger$  ( $b$ ) is the creation (annihilation) operator of the mechanical mode with resonance frequency  $\omega_m$ , and  $g$  is the single-photon optomechanical coupling strength. The parameters  $\Omega_0$  and  $\sqrt{2}\sigma$  are, respectively, the amplitude and duration of the Gaussian wave packets [50].  $t_1 + kT$  ( $t_2 + kT$ ) corresponds to the time instant when the pulse  $\Omega_1(t)$  [ $\Omega_2(t)$ ] reaches its maximum value, where  $k$  is an integer and  $T$  is the time interval of consecutive Gaussian wave packets.

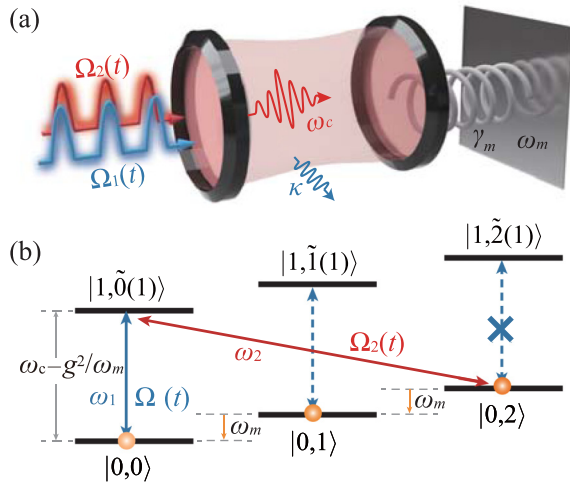


FIG. 1. (a) Schematic diagram of a cavity optomechanical system consisting of a single-cavity mode coupled to a mechanical mode via radiation-pressure interaction. The optical cavity is driven by two Gaussian pulse driving fields  $\Omega_1(t)$  and  $\Omega_2(t)$ . (b) The resonant transition of the effective Hamiltonian  $H_{\text{eff}}^{(2)}$  at the coupling strength  $g/\omega_m \approx 0.765$ , where there is no transition between  $|0, 2\rangle$  and  $|1, \tilde{2}(1)\rangle$ . Other parameters are  $\Delta_1 \equiv \omega_1 - \omega_c = -g^2/\omega_m$  and  $\Delta_2 \equiv \omega_2 - \omega_c = -g^2/\omega_m - 2\omega_m$ .

In the rotating frame with respect to  $\omega_c$ , Hamiltonian (1) becomes

$$H_r = \omega_m b^\dagger b - g a^\dagger a (b^\dagger + b) + [\Omega_1(t) a^\dagger e^{-i\Delta_1 t} + \Omega_2(t) a^\dagger e^{-i\Delta_2 t} + \text{H.c.}], \quad (3)$$

where  $\Delta_1 = \omega_1 - \omega_c$  and  $\Delta_2 = \omega_2 - \omega_c$  are detunings between the carrier frequencies of two pulse driving fields and the cavity frequency, respectively.

By introducing a conditional displacement operator  $D(\beta a^\dagger a) = \exp[\beta a^\dagger a (b^\dagger - b)]$  with  $\beta = g/\omega_m$ , the first two terms  $H_s = \omega_m b^\dagger b - g a^\dagger a (b^\dagger + b)$  of Eq. (3) can be diagonalized as

$$H_s = \sum_{n,m=0}^{\infty} E_{n,m} |n, \tilde{m}(n)\rangle \langle n, \tilde{m}(n)|, \quad (4)$$

where the eigenstates of  $H_s$  are  $|n, \tilde{m}(n)\rangle = |n\rangle_a \otimes |\tilde{m}(n)\rangle_b = |n\rangle_a \otimes D(n\beta)|m\rangle_b$ , and the corresponding eigenvalues are  $E_{n,m} = m\omega_m - g^2 n^2/\omega_m$ . Here  $|n\rangle_a$  ( $n = 0, 1, 2, \dots$ ) are the number states of the cavity mode,  $|m\rangle_b$  ( $m = 0, 1, 2, \dots$ ) are the number states of the mechanical mode, and  $|\tilde{m}(n)\rangle_b$  are the  $n$ -photon displaced number states of the mechanical mode. In particular, when  $n = 0$ , we have  $|0, \tilde{m}(0)\rangle = |0, m\rangle$ .

By using the eigenbasis of the Hamiltonian  $H_s$ , Hamiltonian (3) can be further written as

$$H_r = H_s + \sum_{n,m,q=0}^{\infty} \{A_{m,q}^{(n)} [\Omega_1(t) e^{-i\Delta_1 t} + \Omega_2(t) e^{-i\Delta_2 t}] \times |n, \tilde{m}(n)\rangle \langle n-1, \tilde{q}(n-1)| + \text{H.c.}\}, \quad (5)$$

where we introduce the coefficients  $A_{m,q}^{(n)} = \sqrt{n} {}_b \langle m|D(-\beta)|q\rangle_b$ . The coefficients can be calculated by [51]

$$A_{m,q}^{(n)} = \begin{cases} \sqrt{n} \sqrt{\frac{m!}{q!}} e^{-\frac{\beta^2}{2}} \beta^{q-m} L_m^{q-m}(\beta^2), & m < q \\ \sqrt{n} \sqrt{\frac{q!}{m!}} e^{-\frac{\beta^2}{2}} (-\beta)^{m-q} L_q^{m-q}(\beta^2), & m \geq q \end{cases} \quad (6)$$

where  $L_m^q(x)$  are the associated Laguerre polynomials. In the rotating frame with respect to  $H_s$ , the Hamiltonian (5) is transformed as

$$H_I = \sum_{n,m,q=0}^{\infty} \{A_{m,q}^{(n)} [\Omega_1(t) e^{i(\delta_{n,m,q} - \Delta_1)t} + \Omega_2(t) \times e^{i(\delta_{n,m,q} - \Delta_2)t}] |n, \tilde{m}(n)\rangle \langle n-1, \tilde{q}(n-1)| + \text{H.c.}\}, \quad (7)$$

where the variable  $\delta_{n,m,q} = E_{n,m} - E_{n-1,q} = (m-q)\omega_m - g^2(2n-1)/\omega_m$ .

## III. EFFECTIVE HAMILTONIAN AND GENERATION OF THE TWO-PHONON STATE

In this section, we will derive the effective Hamiltonian for  $H_I$  in a finite-dimensional Hilbert space and analyze the generation of a two-phonon state.

### A. Effective Hamiltonian in a confined Hilbert space

To analyze the generation of  $N$ -phonon states, we derive the effective Hamiltonian for  $H_I$  in a finite-dimensional

Hilbert space. Under the condition of the resolved sideband (i.e., the cavity-field decay rate  $\kappa$  is much smaller than the mechanical frequency  $\omega_m$ ), we choose the driving carrier frequencies  $\omega_1$  and  $\omega_2$  to satisfy the resonance transitions of  $|0, m\rangle \xleftrightarrow{\Omega_1(t)} |1, \tilde{m}(1)\rangle$  and  $|0, m+2\rangle \xleftrightarrow{\Omega_2(t)} |1, \tilde{m}(1)\rangle$ , respectively [see Fig. 1(b)]. Hence, the two driving detunings are  $\Delta_1 = -g^2/\omega_m$  and  $\Delta_2 = -g^2/\omega_m - 2\omega_m$ . In this circumstance, Hamiltonian (7) can be broken down into two parts:

$$H_I = \tilde{H}_I + H'_I, \quad (8)$$

where  $\tilde{H}_I$  denotes the resonant transitions

$$\begin{aligned} \tilde{H}_I = & \sum_{m=0}^{\infty} [\Omega_1(t) A_{m,m}^{(1)} |1, \tilde{m}(1)\rangle \langle 0, m| \\ & + \Omega_2(t) A_{m,m+2}^{(1)} |1, \tilde{m}(1)\rangle \langle 0, m+2|] + \text{H.c.}, \end{aligned} \quad (9)$$

and  $H'_I$  corresponds to the off-resonant transitions

$$\begin{aligned} H'_I = & \sum_{n,m,q=0}^{\infty} \{ A_{m,q}^{(n)} [\Omega_1(t) e^{i\delta_{n,m,q}^{(1)} t} + \Omega_2(t) e^{i\delta_{n,m,q}^{(2)} t}] \\ & \times |n, \tilde{m}(n)\rangle \langle n-1, \tilde{q}(n-1)| + \text{H.c.} \}. \end{aligned} \quad (10)$$

Here the primed summation in Eq. (10) excludes those terms of the Hamiltonian  $\tilde{H}_I$ , and the off-resonance detunings  $\delta_{n,m,q}^{(i)} = \delta_{n,m,q} - \Delta_i$  are given by

$$\delta_{n,m,q}^{(1)} = (m-q)\omega_m - \frac{2g^2}{\omega_m}(n-1), \quad (11a)$$

$$\delta_{n,m,q}^{(2)} = (m-q+2)\omega_m - \frac{2g^2}{\omega_m}(n-1). \quad (11b)$$

Here  $q \neq m$  in Eq. (11a) and  $q \neq m+2$  in Eq. (11b) for  $n=1$ .

In order to neglect the off-resonant transition part  $H'_I$ , the parameter conditions  $|\delta_{n,m,q}^{(i)}| \gg |A_{m,q}^{(n)}| \Omega_0$  ( $i=1, 2$ ) should be satisfied. In particular, in order to ignore  $H'_I$ , we need to block the transitions from one-photon states  $|1, \tilde{m}(1)\rangle$  to two-photon states  $|2, \tilde{m}(2)\rangle$ , and this requires  $|\delta_{2,m,q}^{(i)}| \gg |A_{m,q}^{(2)}| \Omega_0$ . Since the coefficients  $|A_{m,q}^{(2)}| \lesssim 1$ , as shown in Fig. 2(b), the parameter condition is [52]

$$\Omega_0 \ll \left| \frac{2g^2}{\omega_m} - K\omega_m \right| \quad (12)$$

with  $K$  being the nearest integer to  $2(g/\omega_m)^2$ . Hence, when the parameter condition of Eq. (12) is satisfied, the Hamiltonian  $H_I$  can be approximately reduced to  $\tilde{H}_I$ , which describes the resonant transitions between zero-photon states  $|0, m\rangle$  and one-photon states  $|1, \tilde{m}(1)\rangle$ .

In addition, the dimension of the Hilbert space of the mechanical mode can also be approximately truncated up to  $m=N$  by choosing the single-photon optomechanical coupling strength  $g = g_N$ , where  $g_N$  is the minimal positive value satisfying the following equation:

$$A_{N,N}^{(1)} = \exp\left(-\frac{g_N^2}{2\omega_m^2}\right) L_N^0\left(\frac{g_N^2}{\omega_m^2}\right) = 0, \quad (13)$$

with  $N$  being a positive even number. It can be seen from Eq. (13) that the transition matrix element  $\Omega_1(t) A_{N,N}^{(1)}$  from

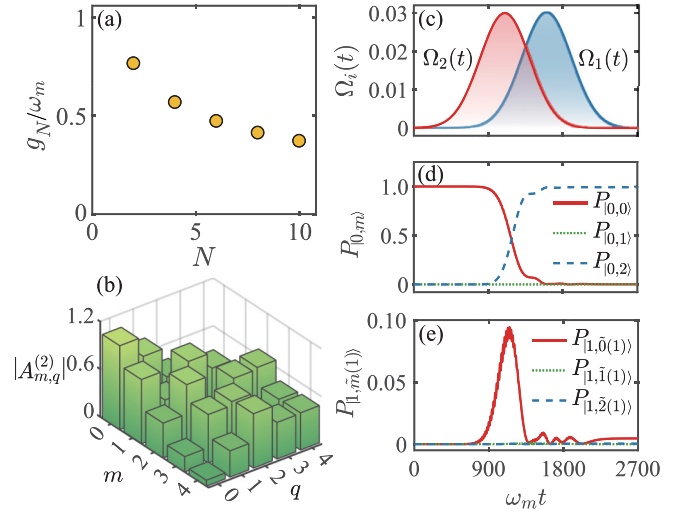


FIG. 2. (a) The ratio  $g_N/\omega_m$  of the minimal positive value  $g_N$  satisfying Eq. (13) over the mechanical frequency  $\omega_m$  as a function of the index  $N$ . (b) The coefficients  $|A_{m,q}^{(2)}|$  as functions of the indices  $m$  and  $q$  at  $g/\omega_m \approx 0.765$ . (c)–(e) The first Gaussian wave packets of two pulse lasers  $\Omega_i(t)$  ( $i=1, 2$ ), the zero-photon state populations  $P_{0,m} = |\langle 0, m | \psi(t) \rangle|^2$ , and the single-photon state populations  $P_{1,\tilde{m}(1)} = |\langle 1, \tilde{m}(1) | \psi(t) \rangle|^2$  as functions of the time  $\omega_m t$ . Here  $|\psi(t)\rangle$  is the state of the system at time  $t$  in the absence of dissipation. Other parameters are  $\Omega_0/\omega_m = 0.03$ ,  $\omega_m \sigma = 300$ ,  $\omega_m t_1 = 1600$ ,  $\omega_m t_2 = 1100$ ,  $g/\omega_m \approx 0.765$ ,  $\Delta_1 = -g^2/\omega_m$ , and  $\Delta_2 = -g^2/\omega_m - 2\omega_m$ .

the state  $|0, N\rangle$  to  $|1, \tilde{N}(1)\rangle$  is zero. In Fig. 2(a), we show the dependence of the ratio  $g_N/\omega_m$  of the minimal positive value  $g_N$  satisfying Eq. (13) over the mechanical frequency  $\omega_m$  on the index  $N$ . The result shows that the coupling strength  $g_N$  decreases as the truncation dimension  $N$  increases.

When the parameter conditions of Eqs. (12) and (13) are satisfied, the effective Hamiltonian of  $H_I$  can be obtained as

$$\begin{aligned} H_{\text{eff}}^{(N)} = & \sum_{m=0}^{N-1} \Omega_1(t) A_{m,m}^{(1)} |1, \tilde{m}(1)\rangle \langle 0, m| + \sum_{m=0}^{N-2} \Omega_2(t) \\ & \times A_{m,m+2}^{(1)} |1, \tilde{m}(1)\rangle \langle 0, m+2| + \text{H.c.}, \end{aligned} \quad (14)$$

where  $H_{\text{eff}}^{(N)}$  describes the resonant transitions between zero-photon states  $|0, m\rangle$  and one-photon states  $|1, \tilde{m}(1)\rangle$  with the phonon number  $m \leq N$ .

## B. Generation of the two-phonon state

We now analyze the generation of the two-phonon state based on technique of STIRAP. When considering the single-photon optomechanical coupling strength  $g/\omega_m = g_2/\omega_m \approx 0.765$ , the dimension of the Hilbert space of the mechanical mode can be truncated up to  $N=2$ , the effective Hamiltonian can then be expressed as

$$\begin{aligned} H_{\text{eff}}^{(2)} = & \Omega_1(t) [A_{0,0}^{(1)} |1, \tilde{0}(1)\rangle \langle 0, 0| + A_{1,1}^{(1)} |1, \tilde{1}(1)\rangle \langle 0, 1|] \\ & + \Omega_2(t) A_{0,2}^{(1)} |1, \tilde{0}(1)\rangle \langle 0, 2| + \text{H.c.} \end{aligned} \quad (15)$$

In Fig. 1(b), we show the resonant transition  $|0, 0\rangle \xleftrightarrow{\Omega_1(t)} |1, \tilde{0}(1)\rangle \xleftrightarrow{\Omega_2(t)} |0, 2\rangle$  of the effective Hamiltonian  $H_{\text{eff}}^{(2)}$ . When

the initial state of the system is  $|0, 0\rangle$ , the transition  $|0, 1\rangle \xleftrightarrow{\Omega_1(t)} |1, \tilde{1}(1)\rangle$  is negligible in the absence of dissipation.

For the effective Hamiltonian  $H_{\text{eff}}^{(2)}$ , the matrix form can be expressed as

$$H_{\text{eff}}^{(2)} = M_{33} \oplus M_{22} \quad (16)$$

with

$$M_{33} = \begin{pmatrix} 0 & \Omega_1(t)A_{0,0}^{(1)} & 0 \\ \Omega_1(t)A_{0,0}^{(1)} & 0 & \Omega_2(t)A_{0,2}^{(1)} \\ 0 & \Omega_2(t)A_{0,2}^{(1)} & 0 \end{pmatrix} \quad (17)$$

and

$$M_{22} = \begin{pmatrix} 0 & \Omega_1(t)A_{1,1}^{(1)} \\ \Omega_1(t)A_{1,1}^{(1)} & 0 \end{pmatrix}. \quad (18)$$

Here the symbol “ $\oplus$ ” denotes the direct sum of the matrix, and the matrix (16) is defined based on the basis states  $|0, 0\rangle = (1, 0, 0, 0, 0)^T$ ,  $|1, \tilde{0}(1)\rangle = (0, 1, 0, 0, 0)^T$ ,  $|0, 2\rangle = (0, 0, 1, 0, 0)^T$ ,  $|0, 1\rangle = (0, 0, 0, 1, 0)^T$ , and  $|1, \tilde{1}(1)\rangle = (0, 0, 0, 0, 1)^T$ , where “ $T$ ” denotes the matrix transpose. Based on the matrices  $M_{33}$  and  $M_{22}$ , we can obtain the eigenvalues of the Hamiltonian  $H_{\text{eff}}^{(2)}$  as

$$\begin{aligned} \varepsilon_0 &= 0, \\ \varepsilon_1 &= -\sqrt{(\Omega_1(t)A_{0,0}^{(1)})^2 + (\Omega_2(t)A_{0,2}^{(1)})^2} = -\varepsilon_2, \\ \varepsilon_3 &= -\Omega_1(t)A_{1,1}^{(1)} = -\varepsilon_4, \end{aligned} \quad (19)$$

and the corresponding eigenstates

$$\begin{aligned} |\phi_0(t)\rangle &= [\Omega_2(t)A_{0,2}^{(1)}|0, 0\rangle - \Omega_1(t)A_{0,0}^{(1)}|0, 2\rangle]/\varepsilon_2, \\ |\phi_1(t)\rangle &= \frac{\Omega_1(t)A_{0,0}^{(1)}|0, 0\rangle - \varepsilon_2|1, \tilde{0}(1)\rangle + \Omega_2(t)A_{0,2}^{(1)}|0, 2\rangle}{\sqrt{2}\varepsilon_2}, \\ |\phi_2(t)\rangle &= \frac{\Omega_1(t)A_{0,0}^{(1)}|0, 0\rangle + \varepsilon_2|1, \tilde{0}(1)\rangle + \Omega_2(t)A_{0,2}^{(1)}|0, 2\rangle}{\sqrt{2}\varepsilon_2}, \\ |\phi_3(t)\rangle &= [|1, \tilde{1}(1)\rangle - |0, 1\rangle]/\sqrt{2}, \\ |\phi_4(t)\rangle &= [|1, \tilde{1}(1)\rangle + |0, 1\rangle]/\sqrt{2}. \end{aligned} \quad (20)$$

Here the eigenstate  $|\phi_0(t)\rangle$  is the so-called dark state, which does not include the component of state  $|1, \tilde{0}(1)\rangle$ . This dark state can also be expressed as  $|\phi_0(t)\rangle = \cos \vartheta(t)|0, 0\rangle - \sin \vartheta(t)|0, 2\rangle$ , where the mixing angle  $\vartheta(t)$  is introduced by  $\tan \vartheta(t) = \Omega_1(t)A_{0,0}^{(1)}/[\Omega_2(t)A_{0,2}^{(1)}]$ . To realize the population transfer from states  $|0, 0\rangle$  to  $|0, 2\rangle$ , the two pulse driving amplitudes  $\Omega_1(t)$  and  $\Omega_2(t)$  should be properly chosen to guarantee adiabatic evolution of  $|\phi_0(t)\rangle$  [47–49]. Concretely, at the beginning of the STIRAP, the relation  $\Omega_1(t)/\Omega_2(t) \rightarrow 0$  should be satisfied such that  $\vartheta(t) = 0$  and  $|\phi_0(t)\rangle \rightarrow |0, 0\rangle$ . At the ending of the STIRAP, the driving amplitudes should satisfy the relation  $\Omega_2(t)/\Omega_1(t) \rightarrow 0$ , then we have  $\vartheta(t) = \pi/2$  and  $|\phi_0(t)\rangle \rightarrow |0, 2\rangle$ . This indicates that the counterintuitive ordering of  $\Omega_1(t)$  and  $\Omega_2(t)$  should be satisfied, i.e.,  $t_1 > t_2$ . In addition, a suitable overlap between the two pulse driving fields is necessary to guarantee adiabatic evolution [49].

To prove the population transfer between the states  $|0, 0\rangle$  and  $|0, 2\rangle$ , we plot the first Gaussian wave packets of the

two pulse driving fields  $\Omega_{1,2}(t)$ , the zero-photon state populations  $P_{|0,m\rangle} = |\langle 0, m | \psi(t) \rangle|^2$ , and the single-photon state populations  $P_{|1,\tilde{m}(1)\rangle} = |\langle 1, \tilde{m}(1) | \psi(t) \rangle|^2$  as functions of the time  $\omega_m t$  in Figs. 2(c)–2(e). Here we consider that the initial state of the system is  $|0, 0\rangle$ , and the two pulse driving fields  $\Omega_{1,2}(t)$  satisfy the condition of STIRAP. It can be seen that the population transfer from state  $|0, 0\rangle$  to  $|0, 2\rangle$  is realized in the absence of the dissipation, i.e., when  $\omega_m t \geq 1800$ , we have  $P_{|0,2\rangle} \approx 1$  and the populations of the other states are approximately zero.

In the realistic physical system, we need to consider the dissipation of the system. In the presence of dissipation, the dynamics of the system can be described by quantum master equation [53]. However, in the ultrastrong-coupling regime [54–56], the dynamics of the system can not be described correctly by the standard quantum master equation. Hence, the dynamics of the system in the ultrastrong-coupling regime should be described by the dressed or generalized master equation [57]. Usually, for a nondegenerate (degenerate) system, the dressed (generalized) master equation can be expressed by the eigensystem of the system Hamiltonian [57]. However, if we know the transformation of the interaction Hamiltonian on the system operator, and the transformed operators correspond to definite-oscillating frequencies so that the secular approximation can be made properly, then we can also obtain the form of the Lindblad operator in the dressed-state representation.

For the cavity optomechanical system described by the Hamiltonian  $H_{\text{opt}} = \omega_c a^\dagger a + \omega_m b^\dagger b - g a^\dagger a (b^\dagger + b)$ , the dissipation of the mechanical mode in the dressed-state representation can be obtained because the transformed operator  $e^{iH_{\text{opt}}t} b e^{-iH_{\text{opt}}t} = e^{-i\omega_m t} (b - \beta a^\dagger a) + \beta a^\dagger a$  can be worked out, and here both  $b - \beta a^\dagger a$  and  $a^\dagger a$  correspond to definite frequency-oscillating terms. However, for the cavity mode, the transformed operator  $e^{iH_{\text{opt}}t} a e^{-iH_{\text{opt}}t} = e^{-i\omega_c t} e^{i\beta^2[\omega_m t - \sin(\omega_m t)](2a^\dagger a + 1)} a e^{\beta[(e^{i\omega_m t} - 1)b^\dagger - (e^{-i\omega_m t} - 1)b]}$  does not correspond to definite-oscillating frequencies. To analyze the oscillating frequency, we need to expand the exponential functions, and then many sidebands are involved. In this case, it is difficult to write out the Lindblad operator of the cavity mode because there exist many complicated transitions. Below, we will make the zero-order approximation with  $e^{i\beta^2[\omega_m t - \sin(\omega_m t)](2a^\dagger a + 1)} a e^{\beta[(e^{i\omega_m t} - 1)b^\dagger - (e^{-i\omega_m t} - 1)b]} \approx a$ , and then the oscillating frequency corresponding to  $e^{iH_{\text{opt}}t} a e^{-iH_{\text{opt}}t}$  is  $\omega_c$ . Under this approximation, we can obtain the Lindblad operator of the cavity mode. For the cavity optomechanical system, this approximation is acceptable because the frequency ( $\sim 10^{14}$  Hz) of the cavity mode is much larger than that ( $\sim 10^7$  Hz) of the mechanical mode. In the derivation of the dressed master equation, we assume that the spectral density of the mechanical bath is of the Ohmic form. In addition, we treat the two pulse driving terms as perturbations.

Under the above approximations, the dressed master equation of the driven optomechanical system in the ultrastrong-coupling regime can be obtained as [58]

$$\begin{aligned} \frac{d\rho(t)}{dt} &= i[\rho(t), H_r] + \gamma_m(n_{\text{th}} + 1)\mathcal{D}[b - \beta a^\dagger a]\rho(t) \\ &\quad + \gamma_m n_{\text{th}}\mathcal{D}[b^\dagger - \beta a^\dagger a]\rho(t) + \kappa\mathcal{D}[a]\rho(t) \\ &\quad + 4\gamma_m(k_B T_b/\omega_m)\beta^2\mathcal{D}[a^\dagger a]\rho(t), \end{aligned} \quad (21)$$

where the Hamiltonian  $H_r$  is given in Eq. (3),  $\kappa$  ( $\gamma_m$ ) is the decay rate of the cavity (mechanical) mode.  $n_{\text{th}} = [\exp(\hbar\omega_m/k_B T_b) - 1]^{-1}$  is the thermal phonon occupation number at temperature  $T_b$ , with  $k_B$  being the Boltzmann constant. The Lindblad superoperators are defined by  $\mathcal{D}[o]\rho(t) = [2o\rho(t)o^\dagger - \rho(t)o^\dagger o - o^\dagger o\rho(t)]/2$ . By numerically solving Eq. (21) [59,60], we can obtain the density operator  $\rho(t)$  of the system at time  $t$ , and then the zero-photon state populations  $P_{|0,m\rangle}(t) = \text{Tr}[|0, m\rangle\langle 0, m|\rho(t)]$  and the single-photon state populations  $P_{|1,\tilde{m}(1)\rangle}(t) = \text{Tr}[|1, \tilde{m}(1)\rangle\langle 1, \tilde{m}(1)|\rho(t)]$  can be calculated.

To be consistent, any physical operator in principle needs to be dressed in the ultrastrong-coupling regime. According to the rules, the annihilation operator  $b$  of the mechanical mode should be replaced by the dressed operator  $b - \beta a^\dagger a$  in the ultrastrong-coupling regime. However, the situation in the present scheme will become simpler based on the following reason. In this scheme, the STIRAP approach is based on the three-level system: the two lower states  $|0, 0\rangle$  and  $|0, 2\rangle$ , the upper state  $|1, \tilde{0}(1)\rangle$ . Since the upper state will not be populated in a perfect STIRAP scheme, the system will mainly be in the two lower states  $|0, 0\rangle$  and  $|0, 2\rangle$ . In realistic simulations, it can be seen from Fig. 2(e) that the population of the single-photon states is smaller than 0.01 during the most duration of the STIRAP, and the peak value of the single-photon-state population is smaller than 0.1, i.e.,  $\langle a^\dagger a \rangle \ll 1$ . This implies that the cavity-field state can be approximated as the vacuum state. In this case, the optomechanical resonator is reduced to a harmonic oscillator described by the operators  $b$  and  $b^\dagger$ . Therefore, it is reasonable to approximately calculate the statistics of the mechanical mode with the operators  $b$  and  $b^\dagger$ .

To study the dynamical evolution of the state populations of the system in the presence of dissipation, we plot the state populations  $P_{|0,m\rangle}(t)$  and  $P_{|1,\tilde{m}(1)\rangle}(t)$  ( $m = 0, 1, 2$ ) as functions of the time  $\omega_m t$  at the optomechanical coupling strength  $g/\omega_m \approx 0.765$ , as shown in Figs. 3(b)–3(d). Similarly, we consider an initial state  $|0, 0\rangle$  of the system, i.e.,  $P_{|0,0\rangle}(0) = 1$ . In Fig. 3(a), we plot the two pulse driving fields  $\Omega_{1,2}(t)$  as a function of the time  $\omega_m t$ . Here we choose the time interval between the consecutive pulses  $\gamma_m T \gg 1$  such that the system goes back to the initial state  $|0, 0\rangle$  before the arrival of the next Gaussian wave packet. In addition, to ensure that the phonons are not dissipated before the completion of the population transfer from the states  $|0, 0\rangle$  to  $|0, 2\rangle$ , the dissipation of the mechanical mode needs to meet  $\gamma_m/\omega_m < 1/1800$  for our used parameters. Meanwhile, the dissipation of the cavity mode should be larger than that of the mechanical mode ( $\kappa > \gamma_m$ ), so that the population of one-photon state is approximately zero. Hence, we employ the experimentally achievable parameters  $\kappa/\omega_m = 0.002$  and  $\gamma_m/\omega_m = 0.0004$  to satisfy these conditions in the numerical simulations. It can be seen from Figs. 3(b)–3(d) that due to the presence of dissipation, the maximal value of the state population  $P_{|0,2\rangle}(t)$  at time  $t = t_s + kT$  is smaller than 1. In addition, due to the decay of the mechanical mode, each phonon in state  $|0, 2\rangle$  is emitted in an intrinsic temporal structure corresponding to the spontaneous emission of the Fock state [20–24,32], the system then goes back to the initial state  $|0, 0\rangle$ . The state  $|0, 2\rangle$  is again generated for the next Gaussian pulse, which means

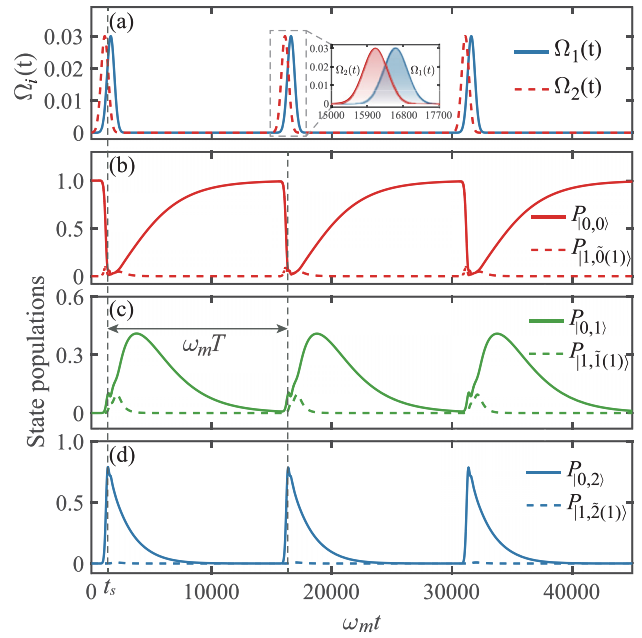


FIG. 3. (a) Two Gaussian pulse driving fields  $\Omega_i(t)$  ( $i = 1, 2$ ) as a function of the time  $\omega_m t$ . (b)–(d) The state populations  $P_{|0,m\rangle}(t)$  and  $P_{|1,\tilde{m}(1)\rangle}(t)$  ( $m = 0, 1, 2$ ) as functions of the time  $\omega_m t$  in the presence of dissipation. Other parameters are  $\Omega_0/\omega_m = 0.03$ ,  $\omega_m \sigma = 300$ ,  $\omega_m t_1 = 1600$ ,  $\omega_m t_2 = 1100$ ,  $\omega_m T = 15000$ ,  $g/\omega_m \approx 0.765$ ,  $\kappa/\omega_m = 0.002$ ,  $\gamma_m/\omega_m = 0.0004$ ,  $T_b = n_{\text{th}} = 0$ ,  $\Delta_1 = -g^2/\omega_m$ , and  $\Delta_2 = -g^2/\omega_m - 2\omega_m$ .

that the dynamical super-Rabi oscillation  $|0, 0\rangle \leftrightarrow |0, 2\rangle$  can be realized under the action of two Gaussian pulse driving fields.

#### IV. DYNAMICAL EMISSION OF PHONON PAIRS

In this section, we study the dynamical emission of phonon pairs and the statistical properties of the dynamical phonon-pair emission. Concretely, we employ the quantum Monte Carlo approach in the ultrastrong-coupling regime [59–61] to simulate individual trajectory of the system. In Figs. 4(a)–4(c), we show a quantum trajectory of the state populations  $P_{|0,m\rangle}(t)$  and  $P_{|1,\tilde{m}(1)\rangle}(t)$  ( $m = 0, 1, 2$ ) at the ratio  $g/\omega_m \approx 0.765$ . Based on the technique of STIRAP, the value of the population  $P_{|0,2\rangle}(t)$  in the state  $|0, 2\rangle$  at time  $t = t_s$  is approximately equal to 1. Due to the trigger of the dissipation of the mechanical mode, the first phonon is emitted (indicated by the first red triangle at the bottom of the figure) and the wave function collapses to the one-phonon state  $|0, 1\rangle$  with almost unit probability, as shown in Fig. 4(b). Immediately, the second phonon is emitted during the mechanical lifetime (the second red triangle), as shown in Fig. 4(a). This means that the strongly correlated phonon pairs are emitted in a very short temporal window and the wave function of the system collapses to the zero-photon state  $|0, 0\rangle$ . After the arrival of the next Gaussian wave packet, the two-phonon state  $|0, 2\rangle$  (the black triangle) is prepared again for the next emission of phonon pairs. Hence, under the action of two Gaussian pulse driving fields, the dynamical emission of phonon pairs can be realized by choosing the appropriate time interval

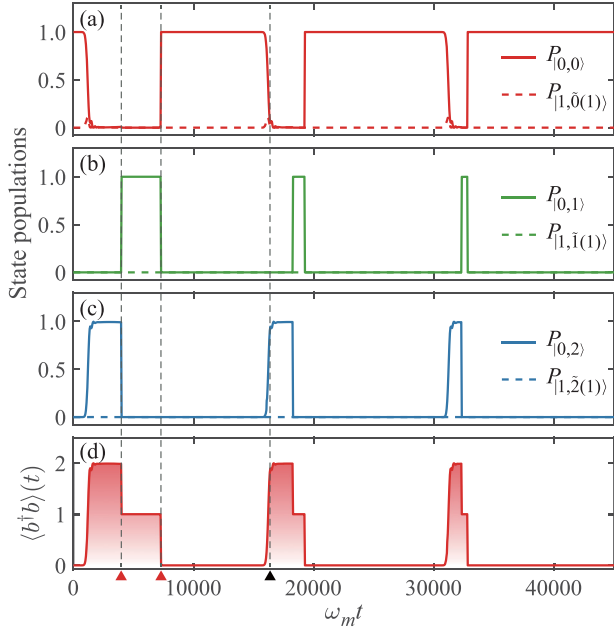


FIG. 4. (a)–(c) Quantum trajectory of the state populations  $P_{|0,m\rangle}(t)$  and  $P_{|1,\bar{m}(1)\rangle}(t)$  ( $m = 0, 1, 2$ ). (d) Quantum trajectory of the average phonon number  $\langle b^\dagger b \rangle(t)$ . Other parameters are  $\Omega_0/\omega_m = 0.03$ ,  $\omega_m\sigma = 300$ ,  $\omega_m t_1 = 1600$ ,  $\omega_m t_2 = 1100$ ,  $\omega_m T = 15000$ ,  $g/\omega_m \approx 0.765$ ,  $\kappa/\omega_m = 0.002$ ,  $\gamma_m/\omega_m = 0.0004$ ,  $T_b = n_{\text{th}} = 0$ ,  $\Delta_1 = -g^2/\omega_m$ , and  $\Delta_2 = -g^2/\omega_m - 2\omega_m$ .

$T$ . Figure 4(d) shows a quantum trajectory of the average phonon number  $\langle b^\dagger b \rangle(t)$  at the ratio  $g/\omega_m \approx 0.765$ . Here we can see that the dynamical cascade-phonon-emission process  $|0, 2\rangle \rightarrow |0, 1\rangle \rightarrow |0, 0\rangle$  occurs in a very short time window.

For the pulse driving fields, we cannot study the steady-state correlation function of the system. Hence, in order to investigate the quantum statistics of the dynamical phonon-pair emission, we numerically calculate the standard and generalized equal-time second-order correlation functions of the mechanical mode [20,23]:

$$g_1^{(2)}(t, t) = \frac{\langle b^\dagger(t)b^\dagger(t)b(t)b(t) \rangle}{\langle b^\dagger b(t) \rangle^2}, \quad (22a)$$

$$g_2^{(2)}(t, t) = \frac{\langle b^{\dagger 2}(t)b^{\dagger 2}(t)b^2(t)b^2(t) \rangle}{\langle b^{\dagger 2}b^2(t) \rangle^2}. \quad (22b)$$

In Fig. 5(a), we display one period of the equal-time second-order correlation functions  $g_N^{(2)}(t, t)$  ( $N = 1, 2$ ) as a function of the time  $\omega_m t$ . It can be seen that the value of the standard correlation function  $g_1^{(2)}(t, t)$  at time  $t = t_{s1}$  is maximum and  $g_1^{(2)}(t_{s1}, t_{s1}) > 1$ , which means that super-Poisson distribution of single phonon occurs at time  $t = t_{s1}$ . Furthermore, we can see that the value of the generalized correlation function  $g_2^{(2)}(t, t)$  at time  $t = t_{s2}$  is minimum and  $g_2^{(2)}(t_{s2}, t_{s2}) < 1$  corresponding to sub-Poisson distribution of phonon pairs.

To further characterize the statistical properties of the dynamical phonon-pair emission, we also numerically calculate the standard and generalized time-delay second-order correlation functions of the mechanical

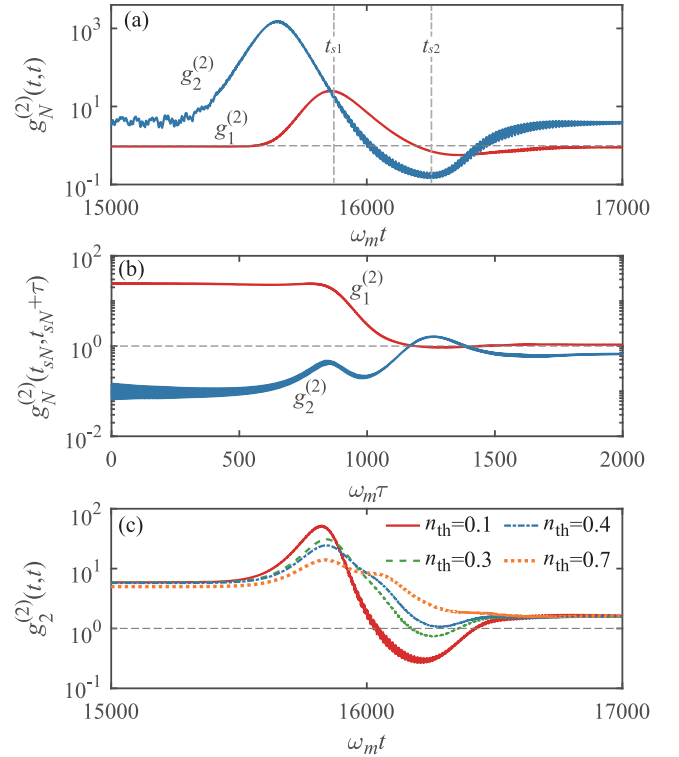


FIG. 5. (a) One period of the equal-time second-order correlation functions  $g_N^{(2)}(t, t)$  as a function of the time  $\omega_m t$  with  $N = 1$  (the red line) and  $N = 2$  (the blue line) at  $T_b = n_{\text{th}} = 0$ . The  $t_{s1}$  and  $t_{s2}$  correspond to the maximum value of  $g_1^{(2)}(t, t)$  and the minimum value of  $g_2^{(2)}(t, t)$ , respectively. (b) The time-delay second-order correlation functions  $g_N^{(2)}(t_{sN}, t_{sN} + \tau)$  ( $t_{s1}$  and  $t_{s2}$  are indicated in the upper panel) with  $N = 1$  (the red line) and  $N = 2$  (the blue line) at  $T_b = n_{\text{th}} = 0$ . (c) One period of the generalized equal-time second-order correlation function  $g_2^{(2)}(t, t)$  as a function of the time  $\omega_m t$  at various values  $n_{\text{th}} = (0.1, 0.3, 0.4, 0.7)$ . Other parameters are  $\Omega_0/\omega_m = 0.03$ ,  $\omega_m\sigma = 300$ ,  $\omega_m t_1 = 1600$ ,  $\omega_m t_2 = 1100$ ,  $\omega_m T = 15000$ ,  $g/\omega_m \approx 0.765$ ,  $\kappa/\omega_m = 0.002$ ,  $\gamma_m/\omega_m = 0.0004$ ,  $\Delta_1 = -g^2/\omega_m$ , and  $\Delta_2 = -g^2/\omega_m - 2\omega_m$ .

mode:

$$g_1^{(2)}(t_{s1}, t_{s1} + \tau) = \frac{G_1^{(2)}(t_{s2}, t_{s2} + \tau)}{\langle b^\dagger b(t_{s1}) \rangle \langle b^\dagger b(t_{s1} + \tau) \rangle}, \quad (23a)$$

$$g_2^{(2)}(t_{s2}, t_{s2} + \tau) = \frac{G_2^{(2)}(t_{s2}, t_{s2} + \tau)}{\langle b^{\dagger 2}b^2(t_{s2}) \rangle \langle b^{\dagger 2}b^2(t_{s2} + \tau) \rangle}. \quad (23b)$$

where  $G_1^{(2)}(t_{s1}, t_{s1} + \tau) = \langle b^\dagger(t_{s1})b^\dagger(t_{s1} + \tau)b(t_{s1} + \tau)b(t_{s1}) \rangle$  and  $G_2^{(2)}(t_{s2}, t_{s2} + \tau) = \langle b^{\dagger 2}(t_{s2})b^{\dagger 2}(t_{s2} + \tau)b^2(t_{s2} + \tau)b^2(t_{s2}) \rangle$ . Figure 5(b) shows the time-delay second-order correlation functions  $g_N^{(2)}(t_{sN}, t_{sN} + \tau)$  for  $N = 1, 2$ , where  $\tau$  is the time delay. Here  $t_{s1}$  and  $t_{s2}$  correspond to, respectively, the times of the maximum value in  $g_1^{(2)}(t, t)$  and the minimum value in  $g_2^{(2)}(t, t)$  in Fig. 5(a). As shown in Fig. 5(b), the numerical result shows that  $g_1^{(2)}(t_{s1}, t_{s1}) > g_1^{(2)}(t_{s1}, t_{s1} + \tau)$  and  $g_2^{(2)}(t_{s2}, t_{s2}) < g_2^{(2)}(t_{s2}, t_{s2} + \tau)$  are satisfied. This means that the two phonons contained in each phonon pair are bunched, but the relation between phonon pairs and phonon pairs is

antibunched, that is, the system behaves as an antibunched phonon-pair emitter.

The above discussions focus on the case of zero temperature, i.e.,  $T_b = 0$  K and  $n_{\text{th}} = 0$ . Below, we will analyze the influence of the thermal phonon occupation number  $n_{\text{th}}$  on the correlation function. In Fig. 5(c), we show the generalized equal-time second-order correlation function  $g_2^{(2)}(t, t)$  as a function of the time  $\omega_m t$  at various values  $n_{\text{th}} = (0.1, 0.3, 0.4, 0.7)$  for the ratio  $g/\omega_m \approx 0.765$ . Here we consider that the initial state of the system is  $|0, 0\rangle$ . It can be seen that the minimum value of the correlation function gradually increases as the thermal phonon number increases. In particular, the value of the correlation function  $g_2^{(2)}(t, t)$  is larger than 1 in the entire parameter space when  $n_{\text{th}} \geq 0.4$ , corresponding to the super-Poisson distribution of phonon pairs. This means that the dynamical phonon-pair emission is destroyed. The reason is that there is a competition between the thermal excitation and the spontaneous radiation of the phonons, and the thermal noise is a vital factor for the destruction of the dynamical emission of phonon pairs in this system.

## V. DISCUSSION AND CONCLUSION

We present some discussions on the experimental parameters in this theoretical scheme. To implement the present physical scheme, the key point is to realize the ultrastrong optomechanical coupling strength. Currently, the strong optomechanical coupling strength (i.e.,  $g/2\pi = 1.6$  MHz) has been realized in a superconducting circuit [62]. In particular, it has been estimated in Ref. [62] that a coupling strength up to  $g/2\pi = 100$  MHz is in principle accessible with an optimized device. In our simulations, we use the following parameters:  $g/\omega_m \approx 0.765$ ,  $\kappa/\omega_m = 0.002$ ,  $\gamma_m/\omega_m = 0.0004$ , and  $\Omega_0/\omega_m = 0.03$  (e.g.,  $\omega_m/2\pi = 100$  MHz,  $g/2\pi = 76.5$  MHz,  $\kappa/2\pi = 0.2$  MHz,  $\gamma_m/2\pi = 0.04$  MHz, and  $\Omega_0/2\pi = 3$  MHz). We want to point out that these parameters are experimentally accessible in a superconducting circuit, but there still exist some challenges for current experimental technology.

In conclusion, we have proposed an efficient scheme to realize the dynamical phonon-pair emission in a cavity op-

tomechanical system, where the optical cavity is driven by two Gaussian pulse driving fields. In the absence of the dissipation of the system, the population transfer from  $|0, 0\rangle$  to  $|0, 2\rangle$  can be realized based on the technique of STIRAP. By studying the quantum trajectories of the state populations and the average phonon number in the system, we found that the dynamical emission of phonon pairs can be observed under appropriate parameter conditions. Particularly, by numerically calculating the standard and generalized second-order correlation functions of the mechanical mode, we found that the cavity optomechanical system can behave as an antibunched phonon-pair emitter when the time interval between the consecutive pulses  $\gamma_m T \gg 1$ . Compared to the previous works of  $n$ -phonon bundle emission [23,25], our work has the following features and advantages. (i) The physical mechanism for creating the two-phonon state is based on the technique of STIRAP, which has not been used in the  $n$ -phonon bundle emission task. (ii) The dynamical phonon-pair emission is tunable on demand with the time interval between the consecutive pulses of pump lasers so that the device behaves as a two-phonon gun, with important applications for on-chip quantum communication. In addition, the phonon-pair emission is realized in a deterministic way. (iii) In this scheme, the probability of the two-phonon state before the phonon emission is much larger than that of the zero- and single-phonon states, then the purity of the dynamical phonon-pair emission will be high. We also note that the present proposal can be extended to achieve an antibunched  $n$ -phonon emitter, which has potential applications in quantum information processing and quantum metrology.

## ACKNOWLEDGMENTS

This work is supported in part by the National Natural Science Foundation of China (Grants No. 12074030, No. U1930402, No. 12175061, No. 11935006, and No. 12147109), the Science and Technology Innovation Program of Hunan Province (Grants No. 2021RC4029, No. 2017XK2018, and No. 2020RC4047), and the China Postdoctoral Science Foundation (Grant No. 2021M700360).

- 
- [1] H. J. Kimble, The quantum internet, *Nature (London)* **453**, 1023 (2008).
  - [2] V. Giovannetti, S. Lloyd, and L. Maccone, Quantum Metrology, *Phys. Rev. Lett.* **96**, 010401 (2006).
  - [3] M. D'Angelo, M. V. Chekhova, and Y. Shih, Two-Photon Diffraction and Quantum Lithography, *Phys. Rev. Lett.* **87**, 013602 (2001).
  - [4] J. C. López Carreño, C. Sánchez Muñoz, D. Sanvitto, E. del Valle, and F. P. Laussy, Exciting Polaritons with Quantum Light, *Phys. Rev. Lett.* **115**, 196402 (2015).
  - [5] K. E. Dorfman, F. Schlawin, and S. Mukamel, Nonlinear optical signals and spectroscopy with quantum light, *Rev. Mod. Phys.* **88**, 045008 (2016).
  - [6] W. Denk, J. H. Strickler, and W. W. Webb, Two-photon laser scanning fluorescence microscopy, *Science* **248**, 73 (1990).
  - [7] N. G. Horton, K. Wang, D. Kobat, C. G. Clark, F. W. Wise, C. B. Schaffer, and C. Xu, In vivo three-photon microscopy of subcortical structures within an intact mouse brain, *Nat. Photonics* **7**, 205 (2013).
  - [8] A. Dousse, J. Suffczynski, A. Beveratos, O. Krebs, A. Lemaître, I. Sagnes, J. Bloch, P. Voisin, and P. Senellart, Ultrabright source of entangled photon pairs, *Nature (London)* **466**, 217 (2010).
  - [9] Y. Ota, S. Iwamoto, N. Kumagai, and Y. Arakawa, Spontaneous Two-Photon Emission from a Single Quantum Dot, *Phys. Rev. Lett.* **107**, 233602 (2011).
  - [10] K. Koshino, K. Inomata, T. Yamamoto, and Y. Nakamura, Implementation of an Impedance-Matched  $\Lambda$  System by Dressed-State Engineering, *Phys. Rev. Lett.* **111**, 153601 (2013).

- [11] G. Callsen, A. Carmele, G. Hönig, C. Kindel, J. Brunmeier, M. R. Wagner, E. Stock, J. S. Reparaz, A. Schliwa, S. Reitzenstein, A. Knorr, A. Hoffmann, S. Kako, and Y. Arakawa, Steering photon statistics in single quantum dots: From one- to two-photon emission, *Phys. Rev. B* **87**, 245314 (2013).
- [12] M. Müller, S. Bounouar, K. D. Jöns, M. Glässl, and P. Michler, On-demand generation of indistinguishable polarization-entangled photon pairs, *Nat. Photonics* **8**, 224 (2014).
- [13] C. S. Muñoz, F. P. Laussy, C. Tejedor, and E. del Valle, Enhanced two-photon emission from a dressed biexciton, *New J. Phys.* **17**, 123021 (2015).
- [14] Y. Chang, A. González-Tudela, C. Sánchez Muñoz, C. Navarrete-Benlloch, and T. Shi, Deterministic Down-Converter and Continuous Photon-Pair Source within the Bad-Cavity Limit, *Phys. Rev. Lett.* **117**, 203602 (2016).
- [15] F. Hargart, M. Müller, K. Roy-Choudhury, S. L. Portalupi, C. Schneider, S. Höfling, M. Kamp, S. Hughes, and P. Michler, Cavity-enhanced simultaneous dressing of quantum dot exciton and biexciton states, *Phys. Rev. B* **93**, 115308 (2016).
- [16] E. Sánchez-Burillo, L. Martín-Moreno, J. J. García-Ripoll, and D. Zueco, Full two-photon down-conversion of a single photon, *Phys. Rev. A* **94**, 053814 (2016).
- [17] X.-L. Dong and P.-B. Li, Multiphonon interactions between nitrogen-vacancy centers and nanomechanical resonators, *Phys. Rev. A* **100**, 043825 (2019).
- [18] P. Bienias, S. Choi, O. Firstenberg, M. F. Maghrebi, M. Gullans, M. D. Lukin, A. V. Gorshkov, and H. P. Büchler, Scattering resonances and bound states for strongly interacting Rydberg polaritons, *Phys. Rev. A* **90**, 053804 (2014).
- [19] M. F. Maghrebi, M. J. Gullans, P. Bienias, S. Choi, I. Martin, O. Firstenberg, M. D. Lukin, H. P. Büchler, and A. V. Gorshkov, Coulomb Bound States of Strongly Interacting Photons, *Phys. Rev. Lett.* **115**, 123601 (2015).
- [20] C. S. Muñoz, E. del Valle, A. G. Tudela, K. Müller, S. Lichtmanecker, M. Kaniber, C. Tejedor, J. J. Finley, and F. P. Laussy, Emitters of  $N$ -photon bundles, *Nat. Photonics* **8**, 550 (2014).
- [21] D. V. Strekalov, A bundle of photons, please, *Nat. Photonics* **8**, 500 (2014).
- [22] C. S. Muñoz, F. P. Laussy, E. del Valle, C. Tejedor, and A. González-Tudela, Filtering multiphoton emission from state-of-the-art cavity quantum electrodynamics, *Optica* **5**, 14 (2018).
- [23] Q. Bin, X.-Y. Lü, F. P. Laussy, F. Nori, and Y. Wu,  $N$ -Phonon Bundle Emission via the Stokes Process, *Phys. Rev. Lett.* **124**, 053601 (2020).
- [24] Q. Bin, Y. Wu, and X.-Y. Lü, Parity-Symmetry-Protected Multiphoton Bundle Emission, *Phys. Rev. Lett.* **127**, 073602 (2021).
- [25] Y. Deng, T. Shi, and S. Yi, Motional  $n$ -phonon bundle states of a trapped atom with clock transitions, *Photonics Res.* **9**, 1289 (2021).
- [26] M. Cosacchi, A. Mielnik-Pyszcorski, T. Seidelmann, M. Cygorek, A. Vagov, D. E. Reiter, and V. M. Axt,  $N$ -photon bundle statistics in different solid-state platforms, [arXiv:2108.03967](https://arxiv.org/abs/2108.03967).
- [27] G. Dfaz-Camacho, E. Z. Casalengua, J. C. L. Carreño, S. Khalid, C. Tejedor, E. del Valle, and F. P. Laussy, Multiphoton Emission, [arXiv:2109.12049](https://arxiv.org/abs/2109.12049).
- [28] J.-F. Huang and C. K. Law, Photon emission via vacuum-dressed intermediate states under ultrastrong coupling, *Phys. Rev. A* **89**, 033827 (2014).
- [29] C. J. Zhu, Y. P. Yang, and G. S. Agarwal, Collective multiphoton blockade in cavity quantum electrodynamics, *Phys. Rev. A* **95**, 063842 (2017).
- [30] Q. Bin, X.-Y. Lü, S.-W. Bin, and Y. Wu, Two-photon blockade in a cascaded cavity-quantum-electrodynamics system, *Phys. Rev. A* **98**, 043858 (2018).
- [31] F. Zou, X.-Y. Zhang, X.-W. Xu, J.-F. Huang, and J.-Q. Liao, Multiphoton blockade in the two-photon Jaynes-Cummings model, *Phys. Rev. A* **102**, 053710 (2020).
- [32] S.-l. Ma, X.-k. Li, Y.-l. Ren, J.-k. Xie, and F.-l. Li, Antibunched  $N$ -photon bundles emitted by a Josephson photonic device, *Phys. Rev. Research* **3**, 043020 (2021).
- [33] A. González-Tudela, V. Paulisch, D. E. Chang, H. J. Kimble, and J. I. Cirac, Deterministic Generation of Arbitrary Photonic States Assisted by Dissipation, *Phys. Rev. Lett.* **115**, 163603 (2015).
- [34] J. S. Douglas, T. Caneva, and D. E. Chang, Photon Molecules in Atomic Gases Trapped Near Photonic Crystal Waveguides, *Phys. Rev. X* **6**, 031017 (2016).
- [35] A. González-Tudela, V. Paulisch, H. J. Kimble, and J. I. Cirac, Efficient Multiphoton Generation in Waveguide Quantum Electrodynamics, *Phys. Rev. Lett.* **118**, 213601 (2017).
- [36] A. Miranowicz, M. Paprzycka, Y.-x. Liu, J. Bajer, and F. Nori, Two-photon and three-photon blockades in driven nonlinear systems, *Phys. Rev. A* **87**, 023809 (2013).
- [37] R. Huang, A. Miranowicz, J.-Q. Liao, F. Nori, and H. Jing, Nonreciprocal Photon Blockade, *Phys. Rev. Lett.* **121**, 153601 (2018).
- [38] W. Qin, V. Macrì, A. Miranowicz, S. Savasta, and F. Nori, Emission of photon pairs by mechanical stimulation of the squeezed vacuum, *Phys. Rev. A* **100**, 062501 (2019).
- [39] K. J. Satzinger, Y. P. Zhong, H.-S. Chang, G. A. Peairs, A. Bienfait, M.-H. Chou, A. Y. Cleland, C. R. Conner, É. Dumur, J. Grebel, I. Gutierrez, B. H. November, R. G. Povey, S. J. Whiteley, D. D. Awschalom, D. I. Schuster, and A. N. Cleland, Quantum control of surface acoustic-wave phonons, *Nature (London)* **563**, 661 (2018).
- [40] Y. Chu, P. Kharel, T. Yoon, L. Frunzio, P. T. Rakich, and R. J. Schoelkopf, Creation and control of multi-phonon Fock states in a bulk acoustic-wave resonator, *Nature (London)* **563**, 666 (2018).
- [41] T. J. Kippenberg and K. J. Vahala, Cavity Optomechanics: Back-Action at the Mesoscale, *Science* **321**, 1172 (2008).
- [42] M. Aspelmeyer, P. Meystre, and K. Schwab, Quantum optomechanics, *Phys. Today* **65**(7), 29 (2012).
- [43] M. Aspelmeyer, T. J. Kippenberg, and F. Marquardt, Cavity optomechanics, *Rev. Mod. Phys.* **86**, 1391 (2014).
- [44] C. K. Law, Interaction between a moving mirror and radiation pressure: A Hamiltonian formulation, *Phys. Rev. A* **51**, 2537 (1995).
- [45] J.-Q. Liao, H. K. Cheung, and C. K. Law, Spectrum of single-photon emission and scattering in cavity optomechanics, *Phys. Rev. A* **85**, 025803 (2012).
- [46] J.-Q. Liao and C. K. Law, Correlated two-photon scattering in cavity optomechanics, *Phys. Rev. A* **87**, 043809 (2013).
- [47] U. Gaubatz, P. Rudecki, S. Schiemann, and K. Bergmann, Population transfer between molecular vibrational levels by stimulated Raman scattering with partially overlapping laser fields. A new concept and experimental results, *J. Chem. Phys.* **92**, 5363 (1990).

- [48] K. Bergmann, H. Theuer, and B. W. Shore, Coherent population transfer among quantum states of atoms and molecules, *Rev. Mod. Phys.* **70**, 1003 (1998).
- [49] N. V. Vitanov, A. A. Rangelov, B. W. Shore, and K. Bergmann, Stimulated Raman adiabatic passage in physics, chemistry, and beyond, *Rev. Mod. Phys.* **89**, 015006 (2017).
- [50] G. H. Hovsepyan and G. Y. Kryuchkyan, Excitations of photon-number states in Kerr nonlinear resonator at finite temperatures, *Eur. Phys. J. D* **69**, 64 (2015).
- [51] F. A. M. de Oliveira, M. S. Kim, P. L. Knight, and V. Buzek, Properties of displaced number states, *Phys. Rev. A* **41**, 2645 (1990).
- [52] G.-F. Xu and C. K. Law, Dark states of a moving mirror in the single-photon strong-coupling regime, *Phys. Rev. A* **87**, 053849 (2013).
- [53] M. O. Scully and M. S. Zubairy, *Quantum Optics* (Cambridge University Press, Cambridge, 1997)
- [54] P. Forn-Díaz, L. Lamata, E. Rico, J. Kono, and E. Solano, Ultrastrong coupling regimes of light-matter interaction, *Rev. Mod. Phys.* **91**, 025005 (2019).
- [55] A. Frisk Kockum, A. Miranowicz, S. De Liberato, S. Savasta, and F. Nori, Ultrastrong coupling between light and matter, *Nat. Rev. Phys.* **1**, 19 (2019).
- [56] A. Le Boité, Theoretical Methods for Ultrastrong Light–Matter Interactions, *Adv. Quantum Technol.* **3**, 1900140 (2020).
- [57] A. Settineri, V. Macrì, A. Ridolfo, O. Di Stefano, A. F. Kockum, F. Nori, and S. Savasta, Dissipation and thermal noise in hybrid quantum systems in the ultrastrong-coupling regime, *Phys. Rev. A* **98**, 053834 (2018).
- [58] D. Hu, S.-Y. Huang, J.-Q. Liao, L. Tian, and H.-S. Goan, Quantum coherence in ultrastrong optomechanics, *Phys. Rev. A* **91**, 013812 (2015).
- [59] J. R. Johansson, P. D. Nation, and F. Nori, QuTiP: An open-source Python framework for the dynamics of open quantum systems, *Comput. Phys. Commun.* **183**, 1760 (2012).
- [60] J. R. Johansson, P. D. Nation, and F. Nori, QuTiP 2: A Python framework for the dynamics of open quantum systems, *Comput. Phys. Commun.* **184**, 1234 (2013).
- [61] V. Macrì, F. Minganti, A. F. Kockum, A. Ridolfo, S. Savasta, and F. Nori, Revealing higher-order light and matter energy exchanges using quantum trajectories in ultrastrong coupling, *Phys. Rev. A* **105**, 023720 (2022).
- [62] J.-M. Pirkkalainen, S. U. Cho, F. Massel, J. Tuorila, T. T. Heikkilä, P. J. Hakonen, and M. A. Sillanpää, Cavity optomechanics mediated by a quantum two-level system, *Nat. Commun.* **6**, 6981 (2015).